



OPEN

Outside-in signaling through the major histocompatibility complex class-I cytoplasmic tail modulates glutamate receptor expression in neurons

Brett A. Eyford^{1,2,3,4,12}, Maciej J. Lazarczyk^{5,6,12}, Kyung Bok Choi^{1,2,3,4,7,8,9}, Merina Varghese⁶, Hitesh Arora^{1,2}, Suresh Kari^{1,2,3,4,7,8,9}, Lonna Munro^{1,2,3,4,7,8,9}, Cheryl G. Pfeifer^{1,2,3,4,7,8,9}, Allison Sowa⁶, Daniel R. Dickstein⁶, Dara L. Dickstein^{6,10,11,13}✉ & Wilfred A. Jefferies^{1,2,3,4,7,8,9,13}✉

The interplay between AMPA-type glutamate receptors (AMPA) and major histocompatibility complex class I (MHC-I) proteins in regulating synaptic signaling is a crucial aspect of central nervous system (CNS) function. In this study, we investigate the significance of the cytoplasmic tail of MHC-I in synaptic signaling within the CNS and its impact on the modulation of synaptic glutamate receptor expression. Specifically, we focus on the Y321 to F substitution (Y321F) within the conserved cytoplasmic tyrosine YXXΦ motif, known for its dual role in endocytosis and cellular signaling of MHC-I. Our findings reveal that the Y321F substitution influences the expression of AMPAR subunits GluA2/3 and leads to alterations in the phosphorylation of key kinases, including Fyn, Lyn, p38, ERK1/2, JNK1/2/3, and p70 S6 kinase. These data illuminate the crucial role of MHC-I in AMPAR function and present a novel mechanism by which MHC-I integrates extracellular cues to modulate synaptic plasticity in neurons, which ultimately underpins learning and memory.

Abbreviations

ΔY	Tyrosine 321 to phenylalanine (Y321F)
AMPA	α-Amino-3-hydroxy-5-methyl-4-isoxazolepropionic acid
CA1	<i>Cornu ammonis</i> 1
CNS	Central nervous system
CREB	Cyclic AMP-responsive element-binding protein

¹Michael Smith Laboratories, The University of British Columbia, 2185 East Mall, Vancouver, BC V6T 1Z4, Canada. ²The Vancouver Prostate Centre, Jack Bell Research Centre, 2660 Oak Street, Vancouver, BC V6H 3Z6, Canada. ³Centre for Blood Research, University of British Columbia, 2350 Health Sciences Mall, Vancouver, BC V6T 1Z3, Canada. ⁴Djavad Mowafaghian Centre for Brain Health, University of British Columbia, 2215 Wesbrook Mall, Vancouver, BC V6T 2B5, Canada. ⁵Division of Institutional Measures, Department of Medical Direction and Quality, University Hospitals of Geneva, Geneva, Switzerland. ⁶Nash Family Department of Neuroscience, Icahn School of Medicine at Mount Sinai, 1425 Madison Ave, New York, NY 10029, USA. ⁷Department of Microbiology and Immunology, University of British Columbia, 1365-2350 Health Sciences Mall, Vancouver, BC V6T 1Z3, Canada. ⁸Department of Zoology, University of British Columbia, 2370-6270 University Blvd., Vancouver, BC V6T 1Z4, Canada. ⁹Department of Medical Genetics, University of British Columbia, 1364-2350 Health Sciences Mall, Vancouver, BC V6T 1Z3, Canada. ¹⁰Department of Pathology, Uniformed Services University of Health Sciences, 4301 Jones Bridge Road, Bethesda, MD 20814, USA. ¹¹The Henry M. Jackson Foundation for the Advancement of Military Medicine (HJF), 6720A Rockledge Drive, Bethesda, MD 20817, USA. ¹²These authors contributed equally: Brett A. Eyford and Maciej J. Lazarczyk. ¹³These authors jointly supervised this work: Dara L. Dickstein and Wilfred A. Jefferies. ✉email: dara.dickstein@usuhs.edu; wilf@msl.ubc.ca

EGFR	Epidermal growth factor receptor
HD	Head diameter
MHC-I	Major histocompatibility complex class I
mTOR	Mechanistic/mammalian target of rapamycin
NMDA	<i>N</i> -Methyl- <i>D</i> -aspartate
PBS	Phosphate-buffered saline
PSD	Post-synaptic density
WT	Wild type

In an unexpected biological twist, major histocompatibility complex class I (MHC-I) molecules have a dual role entwining the immune system with the central nervous system (CNS). In the brain, MHC-I is expressed in neurons under regular physiological conditions^{1–4}. MHC-I plays a role in dendrite morphogenesis and synapse pruning, functions that are considered autonomous from its role in the immune system^{2,5,6}. Indeed, synaptic density was seen to increase when stable surface MHC-I is absent^{2,7–10}, causing impairment in memory and learning^{11–14}. Interestingly, the impact of MHC-I on synaptic density and plasticity, initially thought to occur at early neurodevelopmental stages^{1,2}, can persist throughout life or may re-emerge at an advanced age¹⁰.

The exact mechanism of MHC-I activity and signalling in the CNS remains elusive and has only been studied in the context of genetic loss of MHC-I and associated molecules with the goal of identifying the genes involved in synaptic plasticity. One hypothesis speculates that MHC-I acts in trans by binding putative partner proteins across the synaptic cleft. Indeed, the CD3 ζ and TCR β components of the T-cell receptor, which is the most common MHC-I partner, are expressed in neurons in the CNS^{15,16}. Other known MHC-I binding proteins, such as paired immunoglobulin-like receptor B and Ly49, are also expressed in the CNS and are thought to interact with MHC-I at the synapse^{17,18}. However, mice deficient in these molecules do not recapitulate the phenotype of MHC-I knockout mice^{11,19}, suggesting that MHC-I acts in *cis*. Indeed, MHC-I mediates outside-in or reverse signalling via its intracellular domain²⁰.

Our previous work identified a highly conserved tyrosine residue in the cytoplasmic domain of MHC-I that is required for antigen presentation of exogenously-acquired, but not endogenously-synthesized, antigens in dendritic cells (DCs) to CD8+ Cytotoxic T Lymphocytes (CTLs)²¹. In a mouse model, the conserved tyrosine residue (Y₃₂₁) of MHC-I H-2K^b was substituted with phenylalanine (termed Δ Y). The resultant Δ Y molecules have an impaired ability to internalize from the DC cell surface and cannot traffic to the endolysosomal (LAMP-1 positive) compartments²². As a functional consequence, DCs derived from Δ Y transgenic mice are impaired in their ability to cross-present exogenous sourced protein antigens²³. In addition, Δ Y mice mount inferior CTL responses in vivo upon infection with two viruses that can cause respiratory illnesses²³, vesicular stomatitis virus (VSV) and heat-killed Sendai virus (a classic viral source of exogenous antigen), as well as the intracellular bacteria, *Listeria monocytogenes* that can cause pneumonia²⁴. The Y321F mutation appears to specifically abrogate cross-presentation, as Δ Y DCs are able to efficiently present endogenously-produced protein antigens to specific CTLs in vitro²³.

The conserved Y₃₂₁ residue is part of a conserved YXXA sequence that is highly reminiscent of tyrosine-based YXX Φ endocytic motifs found in other transmembrane proteins (Y is tyrosine, X is any amino acid, A is alanine, and Φ is a bulky, hydrophobic amino acid). Thus, YXXA constitutes an endocytic sorting motif directly responsible for the trafficking of MHC-I through endocytic antigen-loading compartments and ultimately essential for MHC-I antigen cross-presentation and for MHC-I recycling to the cell surface via tyrosine phosphorylation²¹. This is not unique to murine cells as MHC-I has also been observed within endocytic compartments of human DCs, where they acquire exogenous antigens for cross-presentation. The human MHC-I equivalents, human leukocyte antigen-A (HLA-A) and B (HLA-B) molecules, both contain homologous YXXA motifs, suggesting that endocytic trafficking is controlled by similar mechanisms to those used by murine MHC-I. HLA-C lacks the conserved tyrosine residue found in most MHC-I cytoplasmic domains, but trafficking of this molecule is likely to be dependent upon a unique downstream dileucine motif²¹. Therefore, MHC-I molecules recycled from the plasma membrane are a source of loadable MHC-I for participation in antigen cross-presentation^{22,23}. Finally, the cytoplasmic tail of MHC-I also appears to play a role in repressing Toll-like receptor-mediated inflammation²⁰ and other physiological functions²⁵, but no functional studies have been implemented that address its role in the CNS nor the signaling and cellular mechanisms involved with synaptic plasticity.

We recently discovered that the cytoplasmic tail of MHC-I proteins regulates spine and synapse density and morphology in hippocampal neurons. We demonstrated that MHC-I in the CNS functions in *cis* to mediate outside-in function via its intracellular domain, ultimately facilitating synaptic plasticity. In the present study, we aim to provide mechanistic details that could connect MHC-I to its function in neurons. To ascertain the role of the MHC-I cytoplasmic tail in excitatory synaptic function and associated intracellular signalling in the CNS, we examined pre- and post-synaptic protein expression and signaling through kinase activity in hippocampal neurons from a mouse strain expressing a Y321 to F substitution (Y321F) of the conserved cytoplasmic Wild-type (WT) tyrosine (Y321) in the YXX Φ motif of the cytoplasmic tail of MHC-I in animals lacking all other MHC-I molecules.

These experiments thus reveal a novel mechanism of regulation of excitatory signalling in the hippocampus involving MHC-I sensing the external environment to convey information through its cytoplasmic tyrosine-based motif.

Results

The mutated YXX Φ motif alters the level of expression of AMPA receptors at the synapse. We previously observed differences in the spine and synaptic densities and memory in a mouse strain expressing a Y321 to F substitution (Y321F) of the conserved cytoplasmic WT tyrosine (Y321) in the YXX Φ motif of the cytoplasmic tail of MHC-I in animals lacking all other MHC-I molecules²⁶. Here, for simplicity we abbreviate Y321F substitution to ΔY and sought to establish a molecular mechanism to explain our previous observations²⁶. Initially, we examined whether the changes we observed between WT and ΔY mice were associated with alterations in synaptic protein expression. Western blot analysis of pre-synaptic proteins synaptophysin in Fig. 1a ($p=0.15$) and vesicular glutamate transporter 1 (VGLUT1) in Fig. 1b ($p=0.29$) in the hippocampus showed no statistical differences between genotypes.

We also analyzed levels of three post-synaptic proteins: postsynaptic density protein 95 (PSD95), the N-Methyl-D-aspartate (NMDA) receptor GluN2B subunit, and the α -Amino-3-hydroxy-5-methyl-4-isoxazolepropionic acid (AMPA) receptor GluA2/3 subunit in hippocampal homogenates. We did note a significant decrease in GluA2/3 expression in ΔY mice in comparison to WT littermates in Fig. 2a ($p=0.0078$) and no change in GluN2B in Fig. 2b ($p=0.5879$) or PSD95 expression in Fig. 2c ($p=0.1926$).

The ΔY mutation alters the phosphorylation of various kinases and transcription factors. Given the dual-functional role of the YXX Φ motif in both endocytosis and cellular signalling²⁰, we performed an assay to determine which signalling pathways were altered in the ΔY mice as indicated by differential phosphorylation levels of kinases and transcription factors. We found that many kinases and transcription factors were differentially phosphorylated in ΔY mice, as compared to WT controls (Fig. 3a). Phosphorylation of mitogen-activated protein kinases (MAPKs) involved in inflammation was drastically up-regulated. In particular, phosphorylation of p38 α and extracellular signaling regulated kinase 1 (ERK1), which are downstream of MAPK, were up-regulated by 60 and 40 fold respectively. Downstream transcription factors like the immediate early gene c-Jun or transcription factor AP-1, the serine-threonine protein kinase MSK1 or ribosomal protein S6 kinase alpha-5, cyclic AMP-responsive element-binding protein (CREB) and signal transducer and activator of transcription 5A (STAT5a) also showed a drastic increase in their phosphorylation levels, but the increase in levels of STAT2 and STAT6 was not that profound. Non-receptor tyrosine-protein kinases such as Lyn, Lck, Fgr and Fyn of the Src family kinases (SFks) showed up to a 50-fold up-regulation. In contrast, kinases involved in cell survival such as RAC-alpha serine/threonine-protein kinase or Akt1 and ribosomal protein S6 kinase beta-1 or p70S6 kinase exhibited a decrease in phosphorylation. Serine/threonine-protein kinase mechanistic/mammalian target of rapamycin (mTOR) levels remained unchanged and levels of the receptor tyrosine kinase epidermal growth factor receptor (EGFR) increased slightly. Phosphorylation of transcription factor p53 at serine 46 was slightly up-regulated and at serine 15 was 80-fold down-regulated (Fig. 3a). Evidence exists that the p38

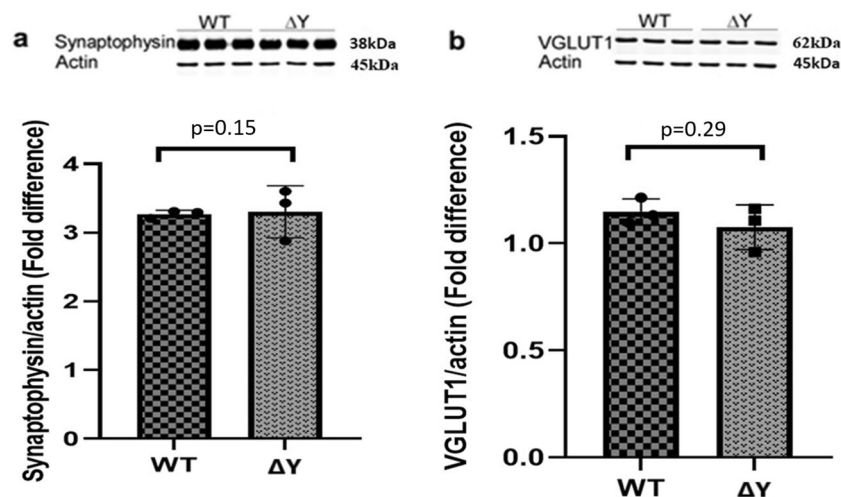


Figure 1. The ΔY mutation has no effect on the expression of pre-synaptic proteins in the hippocampus. Representative Western blots and analysis of integrated fluorescent intensities of pre-synaptic proteins, synaptophysin and VGLUT1, from WT and ΔY mice, $n=3$ independent experiments. Each lane for the Western blots represents a different mouse. The data was pooled from each group in the graphs, and statistical analysis was performed between each group. All proteins were normalized to actin, and values represent means \pm SEM. (a) Synaptophysin has an apparent molecular weight of 38 kDa, and beta-actin has an apparent molecular weight of 45 kDa. There is no statistical difference between protein expression in VGLUT1 expression in ΔY compared to WT mice ($p=0.29$). (b) Based on the standard of molecular weight (MW) markers proteins, VGLUT1 has apparent molecular weight of 62 kDa. There is no statistical difference between protein expression in synaptophysin expression in ΔY compared to WT mice ($p=0.15$) using an unpaired t test. The full-gels and their analysis are provided in the Supplementary figures, including the migration of each protein relative the MW ladder.

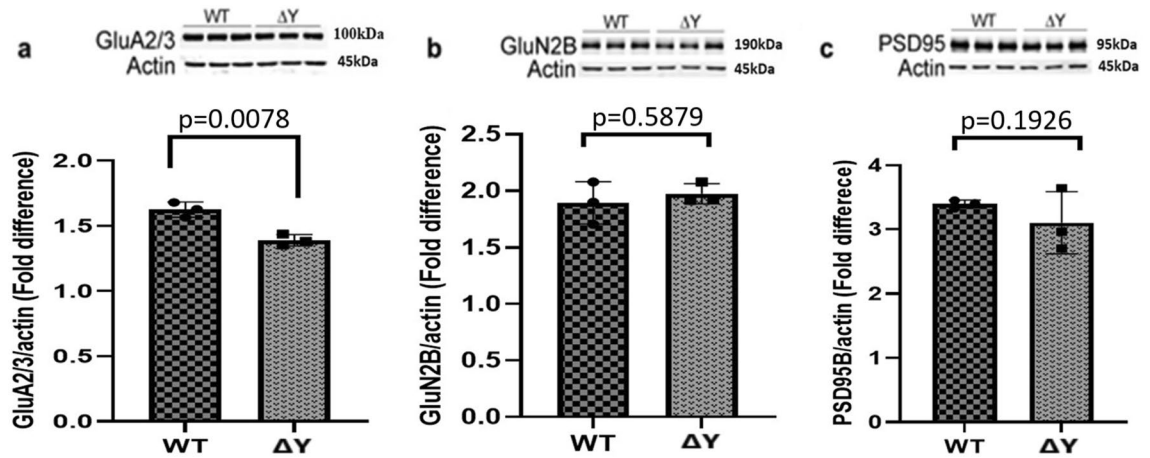


Figure 2. The ΔY mutation reduces the expression of AMPA receptors. Representative Western blots and analysis of integrated fluorescent intensities of post-synaptic proteins GluA2/3, GluN2B, and PSD95 in ΔY and WT mice, $n=3$. (a) There was an observed significant decrease in GluA2/3 in ΔY mice compared to WT mice ($p=0.0078$) using an unpaired t test. (b) No change in GluN2B in ΔY mice compared to WT mice ($p=0.5879$) using an unpaired t test. (c) No changes in PSD95 expression in ΔY mice compared to WT mice ($p=0.1926$) using an unpaired t test. All proteins were normalized to beta-actin and values represent means \pm SEM. Each lane for the western blots represents a different mouse. The data was pooled from each group in the graphs, and statistical analysis was performed between each group. Based on the standard of molecular weight markers, GluA2/3 has an apparent molecular weight of 100 kDa, GluN2b has an apparent molecular weight of 190 kDa, PSD95 has an apparent molecular weight of 95 kDa, and actin has an apparent molecular weight of 45 kDa. The full-gels and their analysis is provided in the Supplementary figures, including the migration of each protein relative to the MW ladder.

MAP kinase pathway dysregulation of MHC-I-expressing monocytic cells correlates with MHC-I misfolding²⁷. Validating the results in the protein array, the phosphorylation levels of p38 in the brain homogenates of ΔY mice was up-regulated compared to WT and representative western blots are shown in Fig. 3a. Results summarizing the averages of 3 experiments are shown in Fig. 3c. There was no significant difference in p38 protein expression between brain tissue lysates from ΔY and WT mice normalized to tubulin ($p=0.1107$), nor as a ratio between ΔY and WT mice ($p=0.0572$). However, a significant difference in phospho-p38 levels normalized to tubulin ($p=0.0001$) and as a ratio between ΔY and WT mice ($p=0.001$) was clearly evident. Overall, the validation studies in Fig. 3b,c are consistent with the phosphoprotein arrays in Fig. 3a showing the phosphorylation of p38 in ΔY mice is statistically greater than in WT brain extracts.

Figure 4 illustrates the major MHC-I signalling pathways that have been established in various immune and non-immune cell types.

Discussion

The mechanisms by which the cytoplasmic tail of MHC-I plays a role in the CNS, in particular how it regulates synaptic function, remain unknown. In the periphery, the cytoplasmic domain of MHC-I is known to be involved in the regulation of signalling events, specifically in the phosphorylation of specific kinases. Furthermore, there is no single or unique disease pathway that these kinases are involved in; on the contrary, the same kinases can be involved in normal cell physiology and signalling across multiple organ systems, including the cardiac, pulmonary, central and peripheral nervous system, as well as in pathological cell functioning associated with multiple diseases and disorders, including cancers, cardiac, pulmonary, neurology, and neurodegeneration, all of which are known to involve one or more of these kinases. However, based on the kinase array data, we have identified putative mechanisms by which this regulation of CNS functions can occur. It is known that the phosphorylation of the Y321 residue on MHC-I results in the recruitment of kinases for intracellular signalling^{29,30}. The kinase array was chosen because it covers kinases involved in oncology, cardiology, pulmonology, and neurobiology and that are considered important in normal cell physiology and disease. This array data revealed a variety of proteins that were differentially phosphorylated in ΔY mice. In particular, we observed changes in proteins implicated in inflammation, survival and growth, such as p38 and ERK1/2, Src, Fyn, Lyn, Lck, Fgr, p70S6 and p53. Of these proteins, we observed increases in the phosphorylation of many members of the Src family kinases (SFK) like Fyn or Lck. In the CNS, SFKs, such as Fyn, Lyn, Lck and Fgr are expressed during development and are implicated in proliferation and differentiation. However, SFKs are also expressed in differentiated neurons in the adult CNS where they regulate ion channel activity, such as NMDA receptors (NMDARs), and synaptic transmission at glutamatergic synapses³¹. Moreover, PSD and SFKs are components of the NMDAR complex (reviewed in³²). This expression pattern and change in function may correspond to MHC-I function as our previous study demonstrated that MHC-I also plays a role in the adult CNS¹⁰. Indeed, Fyn kinase that is hyperphosphorylated is known to play a crucial role in synapse development³³, myelination³⁴, long-term potentiation^{35,36}, learning and memory³⁷⁻³⁹, and NMDA receptor activity⁴⁰. Interestingly, spine density in the hippocampus, while unaltered in

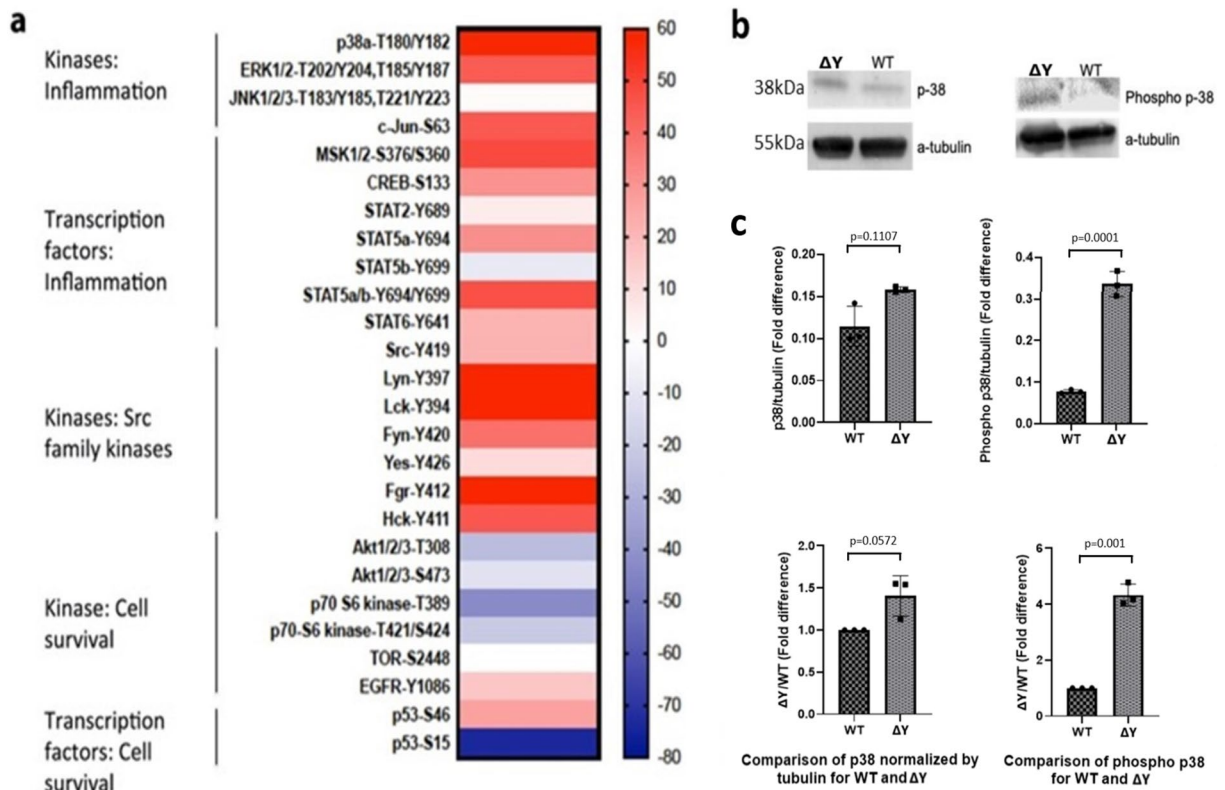


Figure 3. The ΔY mutation alters phosphorylation of various kinases and transcription factors. **(a)** Relative changes in protein kinase phosphorylation levels of target proteins in brain tissue lysates from ΔY and WT mice represented in a heat map as a ratio of the ΔY /WT phosphokinase levels. Increased phosphorylation was observed in various kinases and transcription factors involved in inflammation and members of the Src family kinases with roles in neuronal and synaptic plasticity, while decreased phosphorylation was observed in kinases involved in cell survival. Kinase phosphoarray assays were performed in two animals and analyzed in duplicate in each kinase assay before establishing the means that are shown in the heatmap. **(b)** Validation of the protein phosphoarray by western blot analysis for p38a T180/Y182. Based on the standard molecular weight markers, the control alpha-tubulin has an apparent molecular weight of 55 kDa, and p38 has an apparent molecular weight of 38 kDa. **(c)** Expression levels of phosphorylated and non-phosphorylated p38 in brain tissue lysates from ΔY and WT mice, represented as mean \pm SEM. All comparisons were analyzed using a paired *t* test where $p < 0.05$ was considered significant. The antibodies used were Anti-p38 alpha/MAPK14 antibody, Anti-p38 (phospho T180 + Y182) antibody and Anti-alpha Tubulin antibody. Secondary antibodies: Goat Anti-Mouse IgG H&L (HRP) preabsorbed (ab97040) and Invitrogen. Goat anti-Rabbit IgG (H + L) Secondary Antibody, HRP (31460) The full-gels and their analysis is provided in the Supplementary figures, including the migration of each protein relative the MW ladder.

young Fyn-deficient mice, is significantly decreased in aged Fyn^{-/-} animals⁴¹. Out of necessity our samples were frozen for storage and then thawed before kinase assays were performed.

Previously, Fyn knockout mice were shown to exhibit reduced axonal branching in the cerebellar cortex⁴², decreased spine density in layer V pyramidal neurons⁴¹, as well as shortages in long-term spatial and potentiation learning³⁵, underscoring their functional role in the dendritic compartment. For Fyn to be able to target the dendritic compartment efficiently, it requires the assistance of Tau, a microtubule-associated protein that has been found to be associated with neurodegenerative diseases such as Alzheimer's disease^{43,44}, a process that is aided by interactions of the SH3 domain of Fyn with Tau, as well as the interaction of the SH2 domain of Fyn with tyrosine-phosphorylated Tau^{45,46}. Additionally, the synaptic localization of Tau, as well as Fyn, has been associated with the increased expression of Tau, especially mutant forms of it such as P301L (found in frontotemporal dementia)^{43,44,47}. This topic has been extensively covered by Padmanabhan et al.⁴⁸.

Another mechanism whereby synaptic ultrastructure is modulated involves the expression of the AMPA receptor GluA2/3. We have previously shown that the complete absence of MHC-I results in increased expression of GluN2B but no change in GluA2/3 expression¹⁰. Our finding of decreased GluA2/3 in ΔY MHC-I mice implies that the cytoplasmic domain of MHC-I is involved in the expression of GluA2/3, but not GluN2B, a subunit of the respective receptors. Trafficking of GluA2/3 subunits to the synapse is constitutive and not activity-dependent⁴⁹, and its impact on spine growth and synapse stability is quite complex. Overexpression of GluA2 increases spine length, width and density in hippocampal neurons in vitro⁵⁰. Meanwhile, in vitro knockdown of this receptor subunit results in smaller and fewer spines in hippocampal neurons, whereas in vivo knockout results in

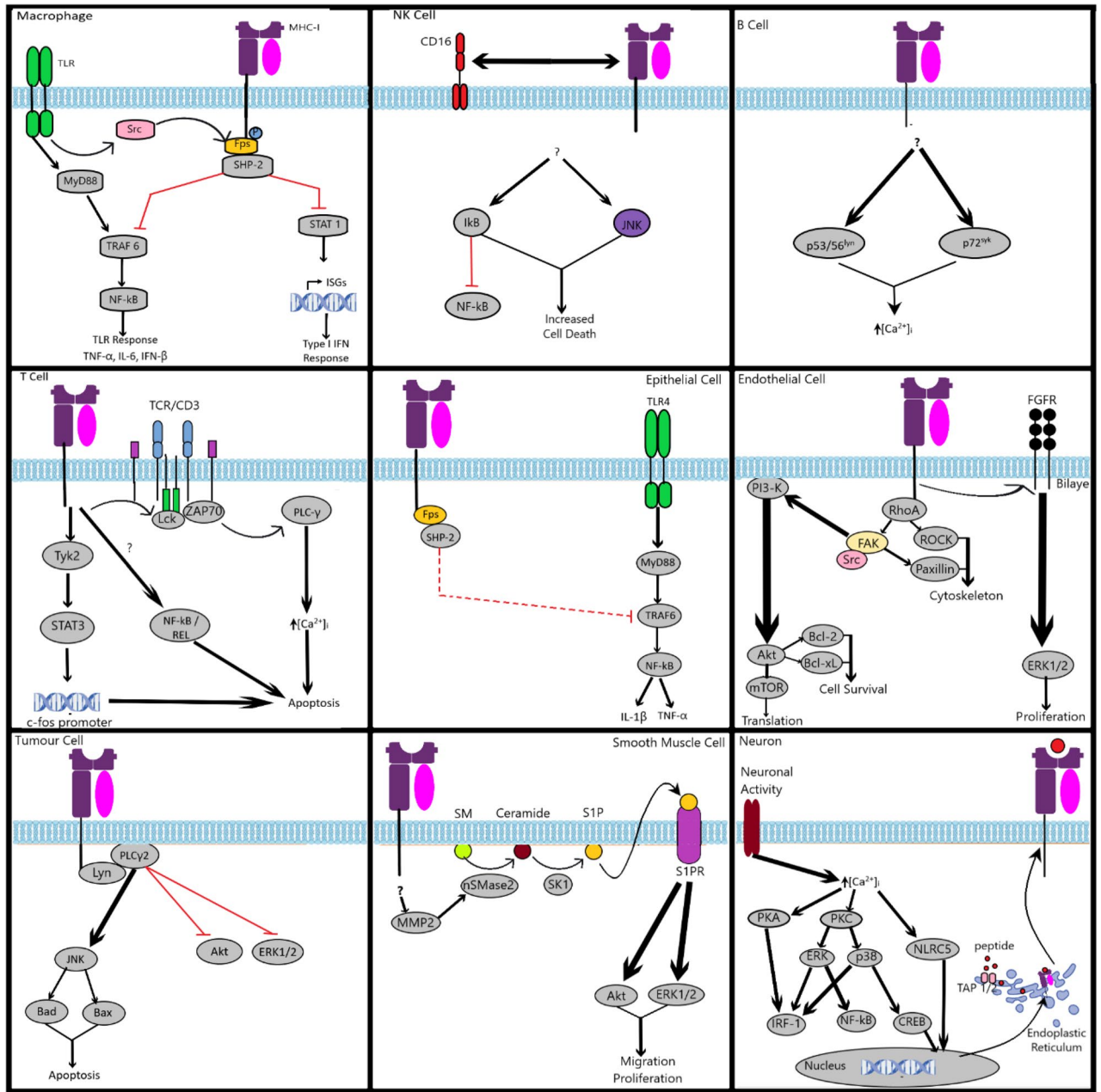


Figure 4. Summary of reverse MHC-I signalling pathways in various cell types. Summary of the main reverse (inside-out) MHC-I signalling pathways in immune and non-immune cells. A more detailed description can be found in a review by Valenzuela and Reed²⁸ as well as Muntjewerff et al.²⁵.

fewer mushroom spines but more thin spines in the dentate gyrus^{50,51}. These reports are in agreement with the decreased GluA2/3 expression and increased thin spines we observed in the hippocampus of ΔY MHC-I mice^{50,51}.

Many intracellular signalling molecules are involved in the regulation of AMPAR expression at the synapse. Some of these proteins include the kinases and transcription factors detected in our array data, such as Lyn, which has been associated previously with AMPARs. In addition to being a ligand-gated ion channel, AMPARs also act as cell-surface signal transducers due to their interaction with Lyn kinase⁵². This interaction facilitates the activation of the MAPK signalling pathway, which includes ERK1/2 and p38, and may contribute to synaptic plasticity and neuroprotection by increasing the expression of neurotrophic factors such as brain-derived neurotrophic factor^{52,53}. By interacting with AMPARs, Lyn kinase phosphorylates the tyrosine residue in the GluA2 subunit of the AMPAR near the C-terminus and regulates AMPAR receptor surface expression and synaptic targeting of GluA2⁵⁴. In our model, we observed a decrease in GluA2/3 expression in ΔY mice and an up-regulation of phosphorylation of Lyn kinase. This follows the relationship above such that as GluA2/3 expression decreases, there is less protein available for Lyn to bind to and become activated, leading to more phosphorylated Lyn kinase and less recycling of GluA2/3^{54,55}. Of the kinases with decreased levels of phosphorylation, p70S6 kinase is a member of the ribosomal s6 kinase family of serine/threonine kinases. In the CNS, it is possible that p70S6

kinase can have an effect on GluA2 expression and neuronal complexity via mTOR, a positive regulator of GluA2 synthesis (reviewed in⁵⁶). A decrease in GluA2/3 via the inhibition of mTOR and p70S6 activity has been implicated in controlling dendritic morphology⁵⁷ and synaptic plasticity^{58,59}. It is possible that the YXXΦ motif in the cytoplasmic tail of MHC-I may be involved in this pathway, given the decrease in GluA2/3 and the decrease in the phosphorylation of p70S6 kinase observed in our study.

Further, recently we demonstrated that the cytoplasmic tail of MHC-I proteins regulates spine and synapse density and morphology in hippocampal neurons, suggesting that synaptic plasticity is facilitated by MHC-I in the CNS functioning in *cis* to mediate outside-in function via its intracellular domain²⁶. It is interesting that there are other existing examples of non-immune cells found to contribute to inflammation promoted by reversing MHC-I signal transduction. For example, bronchiolitis obliterans syndrome develops in patients that have received a lung transplant due to the development of anti-HLA antibodies, which is caused by the activation of airway epithelial cells by HLA-A antibodies⁶⁰. This is accompanied by the production of growth factors (PDGF, HB-EGF, IGF-1, and bFGF), which lead to the proliferation of the fibroblasts, explaining the processes of tissue remodelling and formation of fibrous tissue observed in this phenomenon⁶⁰. Similarly MHC-I outside-in signaling occurs in macrophages where MHC-I was proposed to modulate TLR signaling in epithelial cells, leading to an increase of pro-inflammatory cytokines such as IL-1β and TNF-α⁶¹. In addition, Wu et al.⁶¹ were able to demonstrate that MHC-I cross-linking enhanced the interaction between MHC-I and Fps, while Fps knockdown resulted in decreased levels of SHP-2 and increased cytokine production, indicating that MHC-I on endometrial cells negatively regulates TLR-4-induced inflammatory response by enhancing the Fps-SHP-2 pathway. Thus, outside-in signaling through the MHC-I cytoplasmic domain may have wider impact on physiology than previously considered.

Overall, the present study identifies a mechanism in neurons that allows MHC-I to integrate extracellular cues to mediate neuronal functions in synaptic plasticity. We describe a new pathway integrating the highly conserved tyrosine residue in the cytoplasmic tail of MHC-I in mediating AMPA receptor expression and intracellular signalling via outside-in or reverse signaling. These findings reinforce the importance of a single amino acid on the MHC-I cytoplasmic domain in regulating excitatory neurotransmission in the CNS, opening the door towards modulating MHC-I expression and signalling to modify the function of excitatory synapse function that is intimately connected to learning and memory.

Materials and methods

Experimental animals. The study has been reported in accordance with ARRIVE guidelines⁶² and all mouse experiments were approved by the Animal Care Committee at UBC. We have previously described C3H/He mice carrying the tyrosine mutation on its cytoplasmic tail ($\Delta YK^b C3H$) or expressing transgenic WT MHC-I allele H-2K^b (WTK^bC3H)²³. We crossed H2K^b2D^b double knockout (H2K^{-/-}D^{-/-}) mice with the WTK^bC3H and $\Delta YK^b C3H$ strains, respectively to generate the WTK^b H2D^{-/-} and ΔYK^b H2D^{b/-/-} strains. WTK^bC3H and $\Delta YK^b C3H$ strains were originally maintained on a C3H/He background and express MHC-I genes H2K^k and H2D^k as well as the knocked-in transgenic H-2K^b gene (ΔYK^b or WTK^b). The mice were backcrossed onto an H2K^{-/-}D^{-/-} background (H2K^b2D^b double knockout) for at least 10 generations while the original line was retired. The progeny of the crosses were genotyped by PCR and phenotyped by flow cytometry to establish the presence of MHC-I alleles H2K^k, K^b, D^k and D^b as well as the disrupted H-2K^b and D^b genes. PCR to detect presence of knocked in transgenic H-2K^b (ΔYK^b or WTK^b) used H-2K^b specific oligonucleotides, 5'-TCGCTGAGG TATTTCGTC-3' and 5'-TTGCCCTTGCTTTCTG T-3'⁶³⁻⁶⁵.

Western blotting and kinase array studies were performed on six-month-old mice. Mice were kept under a 12-h light/dark cycle and fed standard lab chow and water ad libitum. All animal experiments were performed at the University of British Columbia, Vancouver, BC, Canada and were conducted in compliance with the University of British Columbia Animal Care Committee under the direction of the Canadian Council for Animal Care.

Western blot. Mouse hippocampi were dissected from WT and ΔY mice (n=3) and were immediately snap-frozen and stored at -80 °C until processed. Hippocampi were homogenized in 2 mL of homogenization buffer (0.32 M sucrose, 1 mM ethylenediaminetetraacetic acid, 1 mg/mL bovine serum albumin, 5 mM 4-(2-hydroxyethyl)-1-piperazineethanesulfonic acid, pH 7.4) using a Dounce homogenizer and immediately mixed 3:5 with 2 × sodium dodecyl sulphate (SDS) sample buffer. Homogenates were separated by SDS polyacrylamide gel electrophoresis followed by transfer to a nitrocellulose membrane (Thermo Scientific, Rockford, IL, USA) as described previously⁶⁶ and were done on 4–15% gradient gel. The primary antibodies used were 1:1000 dilutions of mouse anti-PSD95 (Cat# 75-028, UC Davis/NIH NeuroMab Facility, Davis, CA, USA), mouse anti-GluN2B/NR2B (Cat# 75-101, UC Davis/NIH NeuroMab Facility), goat anti-actin (Cat# sc-1615, Santa Cruz Biotechnology, Santa Cruz, CA, USA) and rabbit anti-GluA2/3 (Cat# AB1506, Millipore, Temecula, CA, USA), mouse primary anti-p38 alpha/MAPK14 antibody (Cat# ab170099 Abcam, Cambridge, UK), anti-p38 (phospho T180 + Y182) antibody (Cat# ab45381 Abcam, Cambridge, UK) and anti-alpha Tubulin antibody (Cat# ab7291 Abcam, Cambridge, UK). The secondary antibodies were 1:10,000 dilutions of AlexaFluor-680 conjugated donkey anti-mouse IgG H + L (Cat# A10038, Life Technologies, Eugene, OR, USA), AlexaFluor-680 conjugated donkey anti-rabbit (Cat# A10043, Life Technologies) and AlexaFluor 790 conjugated donkey anti-goat IgG H + L (Cat# A11370, Life Technologies). Fluorescence was detected and quantitated using Odyssey Infrared Imager (LI-COR, Lincoln, NE, USA). Signal intensities were normalized against β-actin or alpha-tubulin. Results are shown as mean ± SEM.

Phospho-kinase array. Protein kinase phosphorylation levels were measured in hippocampus homogenates (see “Western blot” section for preparation) from ΔY and WT mice using the Proteome Profiler Human

Phospho-Kinase Array kit (ARY003B; R&D SYSTEMS, Minneapolis, MN, USA) according to manufacturer's instructions. The assay is a nitrocellulose membrane-based sandwich ELISA, which has captured antibodies spotted in duplicates on the membrane. The total protein concentration of hippocampal homogenates was measured by Bradford protein assay, and 300 µg of total protein was loaded on the nitrocellulose membrane. The signal intensity from the nitrocellulose membrane, which is proportional to the phosphorylation level of the bound analyte, was measured with the Protein Array Analyzer plugin for ImageJ (NIH, Bethesda, MD, USA). The signal intensity of ΔY samples was normalized to WT, and a heat map was generated depicting the change in phosphorylation intensities using GraphPad Software⁷, Inc. (La Jolla, CA, USA). Results were verified by Western blot using an antibody against tyrosine-protein kinase p38. As a control for the kinase assay, we performed Western blot analysis on p38 since p38 MAP kinase pathway dysregulation of MHC-I-expressing monocytic cells correlates with MHC-I misfolding²⁷. The antibodies used were an anti-p38 alpha/MAPK14 antibody, anti-p38 (phospho T180 + Y182) antibody and anti-alpha Tubulin antibody. Secondary antibodies: Goat Anti-Mouse IgG H&L (HRP) preabsorbed (ab97040) and Invitrogen. Goat anti-Rabbit IgG (H + L) Secondary Antibody, HRP (31460).

Statistical analysis. Unless otherwise stated, all experiments were repeated three times, and the means and statistical significance were determined. The data was then analyzed using the Psych package in RStudio (R version 4.2.0). The resulting summary statistics were used to assess the skewness and kurtosis of data distribution. Shapiro–Wilk and Kolmogorov–Smirnov tests were performed in R to measure the parameters of normal distributions. Normally distributed data were subjected to the appropriate *t* test (unpaired or paired) statistical test (both using GraphPad Prism software, version 9.4.1) with 95% confidence intervals. *P* values less than 0.05 were considered significant. All data were represented as mean ± SEM.

Data availability

The datasets used and/or analyzed during the current study are available from the corresponding author upon reasonable request.

Received: 16 March 2023; Accepted: 12 July 2023

Published online: 11 August 2023

References

- Corriveau, R. A., Huh, G. S. & Shatz, C. J. Regulation of class I MHC gene expression in the developing and mature CNS by neural activity. *Neuron* **21**(3), 505–520 (1998).
- Huh, G. S. *et al.* Functional requirement for class I MHC in CNS development and plasticity. *Science* **290**(5499), 2155–2159 (2000).
- Goddard, C. A., Butts, D. A. & Shatz, C. J. Regulation of CNS synapses by neuronal MHC class I. *Proc. Natl. Acad. Sci. U.S.A.* **104**(16), 6828–6833 (2007).
- Needleman, L. A., Liu, X. B., El-Sabeawy, F., Jones, E. G. & McAllister, A. K. MHC class I molecules are present both pre- and post-synaptically in the visual cortex during postnatal development and in adulthood. *Proc. Natl. Acad. Sci. U.S.A.* **107**(39), 16999–17004 (2010).
- Hu, Y. *et al.* MiR34a regulates neuronal MHC class I molecules and promotes primary hippocampal neuron dendritic growth and branching. *Front. Cell. Neurosci.* **14**, 573208 (2020).
- Shen, Y. *et al.* MHC class I molecules and PirB shape neuronal morphology by affecting the dendritic arborization of cortical neurons. *Neurochem. Res.* **44**(2), 312–322 (2019).
- Glynn, M. W. *et al.* MHCI negatively regulates synapse density during the establishment of cortical connections. *Nat. Neurosci.* **14**(4), 442–451 (2011).
- Dixon-Salazar, T. J. *et al.* MHC class I limits hippocampal synapse density by inhibiting neuronal insulin receptor signaling. *J. Neurosci.* **34**(35), 11844–11856 (2014).
- Lee, H. *et al.* Synapse elimination and learning rules co-regulated by MHC class I H2-Db. *Nature* **509**(7499), 195–200 (2014).
- Lazarczyk, M. J. *et al.* Major histocompatibility complex class I proteins are critical for maintaining neuronal structural complexity in the aging brain. *Sci. Rep.* **6**, 26199 (2016).
- McConnell, M. J., Huang, Y. H., Datwani, A. & Shatz, C. J. H2-K(b) and H2-D(b) regulate cerebellar long-term depression and limit motor learning. *Proc. Natl. Acad. Sci. U.S.A.* **106**(16), 6784–6789 (2009).
- Fourgeaud, L. *et al.* MHC class I modulates NMDA receptor function and AMPA receptor trafficking. *Proc. Natl. Acad. Sci. U.S.A.* **107**(51), 22278–22283 (2010).
- Nelson, P. A. *et al.* MHC class I immune proteins are critical for hippocampus-dependent memory and gate NMDAR-dependent hippocampal long-term depression. *Learn. Mem.* **20**(9), 505–517 (2013).
- Debnath, M., Berk, M., Leboyer, M. & Tamouza, R. The MHC/HLA gene complex in major psychiatric disorders: Emerging roles and implications. *Curr. Behav. Neurosci. Rep.* **5**(2), 179–188 (2018).
- Syken, J. & Shatz, C. J. Expression of T cell receptor beta locus in central nervous system neurons. *Proc. Natl. Acad. Sci. U.S.A.* **100**(22), 13048–13053 (2003).
- Shen, Y. & Zhang, J. Tight regulation of major histocompatibility complex I for the spatial and temporal expression in the hippocampal neurons. *Front. Cell. Neurosci.* **15**, 739136 (2021).
- Zohar, O. *et al.* Cutting edge: MHC class I-Ly49 interaction regulates neuronal function. *J. Immunol.* **180**(10), 6447–6451 (2008).
- Shatz, C. J. MHC class I: An unexpected role in neuronal plasticity. *Neuron* **64**(1), 40–45 (2009).
- Marin, I. A. *et al.* The nonclassical MHC class I Qa-1 expressed in layer 6 neurons regulates activity-dependent plasticity via microglial CD94/NKG2 in the cortex. *Proc. Natl. Acad. Sci.* **119**(23), e2203965119 (2022).
- Xu, S. *et al.* Constitutive MHC class I molecules negatively regulate TLR-triggered inflammatory responses via the Fps-SHP-2 pathway. *Nat. Immunol.* **13**(6), 551–559 (2012).
- Kovacsovics-Bankowski, M. & Rock, K. L. A phagosome-to-cytosol pathway for exogenous antigens presented on MHC class I molecules. *Science* **267**(5195), 243–246 (1995).
- Basha, G. *et al.* MHC class I endosomal and lysosomal trafficking coincides with exogenous antigen loading in dendritic cells. *PLoS One* **3**(9), e3247 (2008).
- Lizee, G. *et al.* Control of dendritic cell cross-presentation by the major histocompatibility complex class I cytoplasmic domain. *Nat. Immunol.* **4**(11), 1065–1073 (2003).
- Reinicke, A. T., Omilusik, K. D., Basha, G. & Jefferies, W. A. Dendritic cell cross-priming is essential for immune responses to *Listeria monocytogenes*. *PLoS One* **4**(10), e7210 (2009).

25. Muntjewerff, E. M., Meesters, L. D., van den Bogaart, G. & Revelo, N. H. Reverse signaling by MHC-I molecules in immune and non-immune cell types. *Front. Immunol.* **11**, 605958 (2020).
26. Lazarczyk, M. J. *et al.* The intracellular domain of major histocompatibility class-I proteins is essential for maintaining excitatory spine density and synaptic ultrastructure in the brain. *Sci. Rep. U.K.* **13**(1), 6448 (2023).
27. Sahlberg, A. S. *et al.* Evidence that the p38 MAP kinase pathway is dysregulated in HLA-B27-expressing human monocytic cells: Correlation with HLA-B27 misfolding. *Arthritis Rheum.* **56**(8), 2652–2662 (2007).
28. Valenzuela, N. M. & Reed, E. F. The link between major histocompatibility complex antibodies and cell proliferation. *Transplant. Rev.* **25**(4), 154–166 (2011).
29. Tscherning, T. & Claesson, M. H. Signal transduction via MHC class-I molecules in T cells. *Scand. J. Immunol.* **39**(2), 117–121 (1994).
30. Santos, S. G., Powis, S. J. & Arosa, F. A. Misfolding of major histocompatibility complex class I molecules in activated T cells allows cis-interactions with receptors and signaling molecules and is associated with tyrosine phosphorylation. *J. Biol. Chem.* **279**(51), 53062–53070 (2004).
31. Omri, B. *et al.* The Lck tyrosine kinase is expressed in brain neurons. *J. Neurochem.* **67**(4), 1360–1364 (1996).
32. Kalia, L. V., Gingrich, J. R. & Salter, M. W. Src in synaptic transmission and plasticity. *Oncogene* **23**(48), 8007–8016 (2004).
33. Maness, P. F. Non-receptor protein tyrosine kinases associated with neuronal development. *Dev. Neurosci.* **14**(4), 257–270 (1992).
34. Sperber, B. R. *et al.* A unique role for Fyn in CNS myelination. *J. Neurosci.* **21**(6), 2039–2047 (2001).
35. Grant, S. G. *et al.* Impaired long-term potentiation, spatial learning, and hippocampal development in Fyn mutant mice. *Science* **258**(5090), 1903–1910 (1992).
36. Kojima, N. *et al.* Rescuing impairment of long-term potentiation in fyn-deficient mice by introducing Fyn transgene. *Proc. Natl. Acad. Sci. U.S.A.* **94**(9), 4761–4765 (1997).
37. Huerta, P. T., Scearce, K. A., Farris, S. M., Empson, R. M. & Prusky, G. T. Preservation of spatial learning in fyn tyrosine kinase knockout mice. *NeuroReport* **7**(10), 1685–1689 (1996).
38. Mizuno, M., Yamada, K., He, J., Nakajima, A. & Nabeshima, T. Involvement of BDNF receptor TrkB in spatial memory formation. *Learn. Mem.* **10**(2), 108–115 (2003).
39. Isosaka, T. *et al.* Activation of Fyn tyrosine kinase in the mouse dorsal hippocampus is essential for contextual fear conditioning. *Eur. J. Neurosci.* **28**(5), 973–981 (2008).
40. Kojima, N., Sakamoto, T., Endo, S. & Niki, H. Impairment of conditioned freezing to tone, but not to context, in Fyn-transgenic mice: Relationship to NMDA receptor subunit 2B function. *Eur. J. Neurosci.* **21**(5), 1359–1369 (2005).
41. Morita, A. *et al.* Regulation of dendritic branching and spine maturation by semaphorin3A-Fyn signaling. *J. Neurosci.* **26**(11), 2971–2980 (2006).
42. Cioni, J.-M. *et al.* SEMA3A signaling controls layer-specific interneuron branching in the cerebellum. *Curr. Biol.* **23**(10), 850–861 (2013).
43. Ittner, L. M. *et al.* Dendritic function of Tau mediates amyloid- β toxicity in Alzheimer's disease mouse models. *Cell* **142**(3), 387–397 (2010).
44. Xia, D., Li, C. & Goetz, J. Pseudophosphorylation of Tau at distinct epitopes or the presence of the P301L mutation targets the microtubule-associated protein Tau to dendritic spines. *Biochim. Biophys. Acta (BBA) Mol. Basis Dis.* **1852**(5), 913–924 (2015).
45. Lee, G., Newman, S. T., Gard, D. L., Band, H. & Panchamoorthy, G. Tau interacts with src-family non-receptor tyrosine kinases. *J. Cell Sci.* **111**(21), 3167–3177 (1998).
46. Bhaskar, K., Yen, S.-H. & Lee, G. Disease-related modifications in Tau affect the interaction between Fyn and Tau. *J. Biol. Chem.* **280**(42), 35119–35125 (2005).
47. Hoover, B. R. *et al.* Tau mislocalization to dendritic spines mediates synaptic dysfunction independently of neurodegeneration. *Neuron* **68**(6), 1067–1081 (2010).
48. Padmanabhan, P., Martínez-Mármol, R., Xia, D., Götz, J. & Meunier, F. A. Frontotemporal dementia mutant Tau promotes aberrant Fyn nanoclustering in hippocampal dendritic spines. *Elife* **8**, e45040 (2019).
49. Shi, S., Hayashi, Y., Esteban, J. A. & Malinow, R. Subunit-specific rules governing AMPA receptor trafficking to synapses in hippocampal pyramidal neurons. *Cell* **105**(3), 331–343 (2001).
50. Passafaro, M., Nakagawa, T., Sala, C. & Sheng, M. Induction of dendritic spines by an extracellular domain of AMPA receptor subunit GluR2. *Nature* **424**(6949), 677–681 (2003).
51. Medvedev, N. I. *et al.* The glutamate receptor 2 subunit controls post-synaptic density complexity and spine shape in the dentate gyrus. *Eur. J. Neurosci.* **27**(2), 315–325 (2008).
52. Hayashi, T., Umemori, H., Mishina, M. & Yamamoto, T. The AMPA receptor interacts with and signals through the protein tyrosine kinase Lyn. *Nature* **397**(6714), 72–76 (1999).
53. Zhang, Q. G. *et al.* Positive modulation of AMPA receptors prevents downregulation of GluR2 expression and activates the Lyn-ERK1/2-CREB signaling in rat brain ischemia. *Hippocampus* **20**(1), 65–77 (2010).
54. Hayashi, T. & Huganir, R. L. Tyrosine phosphorylation and regulation of the AMPA receptor by SRC family tyrosine kinases. *J. Neurosci.* **24**(27), 6152–6160 (2004).
55. Yong, A. J. H. *et al.* Tyrosine phosphorylation of the AMPA receptor subunit GluA2 gates homeostatic synaptic plasticity. *Proc. Natl. Acad. Sci. U.S.A.* **117**(9), 4948–4958 (2020).
56. Switon, K., Kotulska, K., Janusz-Kaminska, A., Zmorzynska, J. & Jaworski, J. Molecular neurobiology of mTOR. *Neuroscience* **341**, 112–153 (2017).
57. Koscielny, A. *et al.* Adaptor complex 2 controls dendrite morphology via mTOR-dependent expression of GluA2. *Mol. Neurobiol.* **55**, 1590–1606 (2018).
58. Cammalleri, M. *et al.* Time-restricted role for dendritic activation of the mTOR-p70S6K pathway in the induction of late-phase long-term potentiation in the CA1. *Proc. Natl. Acad. Sci. U.S.A.* **100**(24), 14368–14373 (2003).
59. Antion, M. D., Hou, L., Wong, H., Hoeffler, C. A. & Klann, E. mGluR-dependent long-term depression is associated with increased phosphorylation of S6 and synthesis of elongation factor 1A but remains expressed in S6K-deficient mice. *Mol. Cell. Biol.* **28**(9), 2996–3007 (2008).
60. Jaramillo, A. *et al.* Anti-HLA class I antibody binding to airway epithelial cells induces production of fibrogenic growth factors and apoptotic cell death: A possible mechanism for bronchiolitis obliterans syndrome. *Hum. Immunol.* **64**(5), 521–529 (2003).
61. Wu, H. *et al.* IFN- τ mediated control of bovine major histocompatibility complex class I expression and function via the regulation of bta-miR-148b/152 in bovine endometrial epithelial cells. *Front. Immunol.* **9**, 167 (2018).
62. Percie du Sert, N. *et al.* The ARRIVE guidelines 2.0: Updated guidelines for reporting animal research. *PLoS Biol.* **18**(7), e3000410 (2020).
63. Perarnau, B. *et al.* Single H2Kb, H2Db and double H2KbDb knockout mice: Peripheral CD8+ T cell repertoire and anti-lymphocytic choriomeningitis virus cytolytic responses. *Eur. J. Immunol.* **29**(4), 1243–1252 (1999).
64. Gustafsson, J. R. *et al.* DNMT1 regulates expression of MHC class I in post-mitotic neurons. *Mol. Brain* **11**(1), 36 (2018).
65. Lin, K. *et al.* MHC class I H2-Kb negatively regulates neural progenitor cell proliferation by inhibiting FGFR signaling. *PLoS Biol.* **19**(6), e3001311 (2021).
66. Beecroft, R. P., Roditi, I. & Pearson, T. W. Identification and characterization of an acidic major surface glycoprotein from procyclic stage *Trypanosoma congolense*. *Mol. Biochem. Parasitol.* **61**(2), 285–294 (1993).

Acknowledgements

BAE is the recipient of a Centre for Blood Research Post-Doctoral Research Fellowship and a Michael Smith Post-doctoral Research Fellowship. MJL was the recipient of a scientific fellowship from the University Hospitals of Geneva and the Vachoux Foundation. HA is the recipient of a Centre for Blood Research Doctoral Research Scholarship. This work was supported by grants from the Canadian Institutes of Health Research (MOP-77631 and MOP-86739 to WAJ). We would like to thank the members of the Dickstein and Jefferies laboratories for technical assistance and discussions and Drs Eliana Al Haddad and Giorgia Caspani for aid in editing the manuscript.

Disclaimer

The opinions expressed herein are those of the authors and are not necessarily representative of those of the government of the United States, the Uniformed Services University of the Health Sciences, the Department of Defense (DoD), or the United States Army, Navy or Air Force or the Henry M. Jackson Foundation for the Advancement of Military Medicine Inc.

Author contributions

D.L.D. and W.A.J. conceived the study and secured funding. W.A.J. provided the animals used in the study. B.A.E., M.J.L., K.B.C., H.A., A.S., D.R.D., and D.L.D. performed the experiments and W.A.J., C.G.P., L.M., M.J.L., B.A.E., K.B.C., H.A., A.S., D.R.D., and D.L.D. analyzed the data. B.A.E., M.J.L., M.V., H.A., C.G.P., W.A.J. and D.L.D. wrote the manuscript. C.G.P., and L.M. provided expertise and feedback on the manuscript. All authors reviewed and edited the manuscript. W.A.J. revised the manuscript.

Competing interests

The authors declare no competing interests.

Additional information

Supplementary Information The online version contains supplementary material available at <https://doi.org/10.1038/s41598-023-38663-z>.

Correspondence and requests for materials should be addressed to D.L.D. or W.A.J.

Reprints and permissions information is available at www.nature.com/reprints.

Publisher's note Springer Nature remains neutral with regard to jurisdictional claims in published maps and institutional affiliations.



Open Access This article is licensed under a Creative Commons Attribution 4.0 International License, which permits use, sharing, adaptation, distribution and reproduction in any medium or format, as long as you give appropriate credit to the original author(s) and the source, provide a link to the Creative Commons licence, and indicate if changes were made. The images or other third party material in this article are included in the article's Creative Commons licence, unless indicated otherwise in a credit line to the material. If material is not included in the article's Creative Commons licence and your intended use is not permitted by statutory regulation or exceeds the permitted use, you will need to obtain permission directly from the copyright holder. To view a copy of this licence, visit <http://creativecommons.org/licenses/by/4.0/>.

© The Author(s) 2023